JYP

3D-QSAR Studies of NAIMS Analogs as anti-HIV Agents

Ganguly S, Prasanthi N

Department of Pharmaceutical Sciences, Birla Institute of Technology, Mesra, Ranchi-835 215, Jharkhand, India

Address for correspondence: *Dr. Swastika Ganguly; E-mail: swastikaganguly@bitmesra.ac.in*

ABSTRACT

Human immunodeficiency virus (HIV) is the causative agent of acquired immunodeficiency syndrome (AIDS), a disease which has claimed twenty million lives worldwide in the last two decades. Recently imidazole derivatives, such as N-aminoimidazoles (NAIMS), have been discovered as novel anti-HIV agents. Herein, the results of comparative molecular field analysis (CoMFA) and comparative molecular similarity indices (CoMSIA) analysis on these inhibitors have been reported. The CoMFA model produced statistically significant results with cross-validated, conventional, and predictive correlation coefficients of 0.517, 0.965, and 0.47, respectively. The combination of electrostatic hydrophobic and donor fields in CoMSIA gave the best results with cross-validated, conventional and predictive correlation coefficients of 0.532, 0.930, and 0.80, respectively. The information obtained from CoMFA and CoMSIA models may be utilized in the design of more potent NAIMS analogs and anti-HIV agents.

Key words: Acquired immune deficiency syndrome, comparative molecular field analysis, comparative molecular similarity indices, human immunodeficiency virus, N-aminoimidazoles, 3D-QSAR

DOI: 10.4103/0975-1483.57074

INTRODUCTION

Human immunodeficiency virus (HIV) is the causative agent of acquired immune deficiency syndrome (AIDS), a disease which has claimed twenty million lives worldwide in the last two decades.[1] Though considerable progress has been made towards the chemotherapy of HIV infection, the hard fact remains that there has been no permanent cure for AIDS till date. Thus, novel anti-HIV drugs are needed worldwide and therefore a search for novel anti-HIV agents with newer mechanisms of action has become an extremely important subject of investigation.

Compounds containing imidazole nucleus have shown a variety of pharmacological actions and many of them have gained worldwide acceptance in clinical practice.[2–5] Recently imidazole derivatives such as N-aminoimidazoles (NAIMS), have been discovered as novel anti-HIV agents which have been found to function either through the classical nonnucleoside reverse transcriptase inhibitor (NNRTI) type of action or through an unknown mode of action which may be someway related to inhibition of immediate post integration or early transcription step.[1,6]

Comparative molecular field analysis (CoMFA) and comparative molecular similarity indices analysis (CoMSIA) are powerful tools to build and design a quantitative structure activity relationship (QSAR) model for a given set of molecules in rational drug design and related applications.[7–9] CoMFA methodology is based on the assumption that the changes in the biological activity correlate with the changes in the steric and electrostatic

fields of the molecules.[9] The CoMSIA[9,10] method differs by the way the molecular fields are calculated and by including additional molecular fields, such as lipophilic and hydrogen bond potential. It has several advantages over CoMFA such as greater robustness regarding both region shift and small shift within the alignments, no arbitrary cut-off and more intuitively interpretable contour maps.

The three dimensional quantitative structure activity relationship (3D-QSAR) studies of NAIMS have been recently reported by taking the cytotoxicity data as dependent variable.[11] However, as the cytotoxicity data is the micromolar concentration of the compounds required to reduce MT-4 cell viability by 50%, and the fact that NAIMS analogs have an unknown mechanism of action, we thought it justifiable to report the CoMFA and CoMSIA studies considering the IC_{50} values of HIV-1 IIIB strain as the dependent parameter. The results of CoMFA and CoMSIA models generated by us provide a rationale for the design of more selective and potent NAIMS analogs as potent anti-HIV agents.

MATERIALS AND METHODS

Dataset

Reported data on a series of 54 NAIMS analogs[6] were used [Table 1]. The IC_{50} data were used for QSAR analysis as a dependent parameter after converting reciprocal of the logarithm of IC_{50} (pIC_{50}) values. IC_{50} is the concentration required to inhibit the viral cytopathic effect by 50% in MT-4 cells. The total set of NAIMS analogs (54 compounds) was divided into a training set of forty five and a test set of nine compounds at random with bias given to structural diversity in both the training set and the test set. The ratio of training set molecules to test set molecules was in the approximate ratio 5:1.

Molecular modeling

The 3D-QSAR was performed using SYBYL 7.1[12] installed on a Dell computer with Red Hat Linux Enterprise Version 3.0 (with 512 MB of memory).The initial conformation of the most active analog 13 was obtained from simulated annealing as it enables the rapid identification of the global minimum energy conformer.[8,12] The system was subjected to simulated annealing by heating at 1000 K for 1 ps and then cooling at 200 K for 1 ps. The exponential annealing function was used and 50 such cycles were run. The least energy conformer obtained by this method was subjected to further minimization. The minimized conformer, thus obtained, was taken as the template and rest of the molecules were built from it. A constrained minimization followed by full minimization was carried out on these molecules in order to prevent the conformations moving to a false region. Tripos force field and partial atomic charges calculated by the Gasteiger-Huckel method were used. Powell's conjugate gradient method was used for minimization. The gradient of 0.05 kcal mol^{-1} $A^{\circ -1}$ was set as a convergence criterion.

Alignment

The superimposition of the molecules is one of the most crucial steps in CoMFA, and the results of CoMFA analysis depend on the alignment of the molecules. The template molecule 13 was taken and the rest of the molecules were aligned to it using the DATABASE ALIGNMENT method in the SYBYL. The molecules were aligned to the template molecule by using common substructure labeled with * in Figure 1. The aligned molecules are shown in Figure 2.

CoMFA interaction energy calculation[9]

The steric and electrostatic CoMFA fields were calculated at each lattice intersection of a regularly spaced grid of 2.0 A° in all three dimensions within defined region. The van der Waals potential and coulombic terms representing the steric and electrostatic fields respectively were calculated using standard Tripos force fields. A distance-dependent dielectric constant of 1.00 was used. An sp3 carbon atom with +/1.00 charge was used as a probe atom. The steric and electrostatic fields were truncated at +/30.00 kcal mol^{-1}, and the electrostatic fields were ignored at the lattice points with maximal steric interactions.

CoMSIA interaction energy calculation[9]

The steric, electrostatic, hydrophobic, hydrogen bond donor and hydrogen bond acceptor potential fields were calculated at each lattice intersection of a regularly spaced grid of 2.0 A °. A probe atom with radius 1.0 A ° and +/1.0 charge with hydrophobicity of +/1.0 and hydrogen bond donor and hydrogen bond acceptor properties of +/1.0 was used to calculate steric, electrostatic, hydrophobic, donor and acceptor fields. The contribution from these descriptors was truncated at 0.3 kcal mol^{-1}.

Partial least square analysis[9]

PLS method was used to linearly correlate the CoMFA fields to the inhibitory activity values. The cross-validation [7,9] analysis was performed using the leave one out (LOO) method in which one compound is removed from the dataset and its activity is predicted using the model derived

Table 1: Dataset used for 3D-QSAR Analyses

Compd. No.	Substituents				IC50 b(μM)
	R1	R2	R3	R4	
1	3-Cl- C_6H_4	SH	CH_3	C_6H_5	6.39±0.94
2	4-F- C_6H_4	SH	CH_3	C_6H_5	>220.13
3	4-Cl- C_6H_4	SH	CH_3	C_6H_5	>134.41
4	3-Cl- C_6H_4	SH	CH_3	3-Br- C_6H_4	8.54±1.06
5	3-Cl- C_6H_4	SH	CH_3	4-Br-C_6H_4	>33.24
6	3-Cl- C_6H_4	SH	CH_3	3-Cl-C_6H_4	5±1.17
7	3-Cl- C_6H_4	SH	CH_3	4-Cl-C_6H_4	>40.80
8	3-Cl- C_6H_4	SH	CH_3	4- CH_3O-C_6H_4	>38.09
9	3-Cl- C_6H_4	SH	C_6H_5	CH_3	49.96
10	3-Cl- C_6H_4	SH	-$(CH_2)_4$-	>126.42	
11	3-Br-C_6H_4	SH	CH_3	C_6H_5	9.96±1.61
12	3- NO_2- C_6H_4	SH	CH_3	C_6H_5	7.29±1.53
13	3-CH_3- C_6H_4	SH	CH_3	C_6H_5	1.56±0.61
14	3-Cl- C_6H_4	SH	CH_3	CH_3	>259.42
15	C_6H_5	SH	CH_3	CH_3	>180.79
16	3- CH_3- C_6H_4	SH	$(CH_3)_2CH$	C_6H_5	>42.63
17	3-Cl- C_6H_4	SH	CH_3 CH_2	C_6H_5	9.06±1.55
18	3- CH_3- C_6H_4	SH	CH_3 CH_2	C_6H_5	17.64±13.02
19	3-Cl- C_6H_4	SH	C_5H_5	C_6H_5	>36.38
20	3-Cl- C_6H_4	SH	CH_3OCO	CH_3	>48.86
21	3- CH_3--5-CH_3- C_6H_3	SH	CH_3	C_6H_5	1.03±0.58
22	3- CH_3O- C_6H_4	SH	CH_3	C_6H_5	4.78±1.38
23	3-Cl- C_6H_4	SH	CH_3	3-CN-C_6H_4	≥99.40
24	3-CH_3- C_6H_4	SH	CH_3	3- CN -C_6H_4	>45.63
25	3-Cl- C_6H_4	SH	CH_3	3-HOCO- C_6H_4	>120.03
26	3-CH_3- C_6H_4	SH	CH_3	3-HOCO-C_6H_4	>187.13
27	3-Cl- C_6H_4	SH	CH_3	3-NH_2CO-C_6H_4	>42.16
28	1-Naphthyl	SH	CH_3	C_6H_5	5.55±2.14
29	4-CH_3CH_2- C_6H_4	SH	CH_3	C_6H_5	>34.45
30	4-CH_3S- C_6H_4	SH	CH_3	C_6H_5	>53.04
31	3-Cl- C_6H_4	H	CH_3	C_6H_5	1.59±0.32
32	3-Cl- C_6H_4	H	CH_3	3-Br-C_6H_5	0.58±0.08
33	3-Cl- C_6H_4	H	CH_3	3-Cl- C_6H_4	0.72±0.59
34	3-Cl- C_6H_4	H	-$(CH_2)_4$-	>67.29	
35	C_6H_5	H	CH_3	C_6H_5	≥11.67
36	3-Cl- C_6H_4	H	CH_3	CH_3	>213.68
37	3- CH3- C_6H_4	H	CH_3	C_6H_5	3.26±0.91
38	4-F- C_6H_4	H	CH_3	C_6H_5	>30.82
39	3-CH_3-C_6H_4	H	CH_3 CH_2	C_6H_5	>27.87
40	3- CH_3-5-CH_3- C_6H_3	H	CH_3	C_6H_5	>20.44
41	3- CH_3O- C_6H_4	H	CH_3	C_6H_5	>34.44
42	3-Cl- C_6H_4	H	CH_3	3-CN-C_6H_4	6.96±2
43	3- CH_3- C_6H_4	H	CH_3	3-CN-C_6H_4	>34.70
44	3- CH_3-C_6H_4	H	CH_3	3-NH_2CO-C_6H_4	>162.39
45	3-Cl- C_6H_4	H	CH_3	3CH_3OCO-C_6H_4	>33.15
46 a	2-Cl-5-Cl- C_6H_3	H	CH_3	C_6H_5	>147.12
47 a	3- CH_3- C_6H_4	H	CH_3	CH_3	>359.86
48 a	3-Cl- C_6H_4	H	CH_3	CH_3OCO	>190.31
49 a	3-Cl- C_6H_4	H	CH_3	3-CH_3OCO-C_6H_4	>67.36
50 a	C_6H_5	H	CH_3	CH_3	>351.42
51 a	3- CH_3- C_6H_4	H	CH_3	CH_3	>20.44
52 a	3-Cl- C_6H_4	H	CH_3	CH3OCO	>34.44
53 a	3-Cl- C_6H_4	H	CH_3	3-NH2 CO -C6H4	>260.50
54 a	3-Cl- C_6H_4	H	CH_3	3-HOCO-C6H4	>160.57

[a]Test set compounds, [b]IC50 is the concentration required to inhibit the viral cytopathic effect by 50% in MT-4 cells.

from the rest of the dataset. The cross-validated r^2 that resulted in optimum number of components and lowest standard error of prediction was taken for further analysis. Equal weights were assigned to steric and electrostatic fields using COMFA_STD scaling option. To speed up the analysis and reduce noise, a minimum filter value σ of 2.00 kcal mol^{-1} was used. Final analysis was performed to calculate conventional r^2 using the optimum number of components. To further assess the robustness and statistical confidence of the derived models, bootstrapping analysis for 100 runs was performed. Bootstrapping[7] is based on simulating a larger number of data sets sampled from the

Table 2: Summary of CoMFA and CoMSIA Statistics

Parameters	CoMFA	CoMSIA		
		EHD Model 1	SEHD Model 2	SED Model 3
r^2_{cv}	0.517	0.532	0.514	0.522
N	6	6	6	6
r^2	0.965	0.930	0.929	0.910
SEE	0.133	0.188	0.19	0.213
F-test value	174.102	84.280	82.964	64.425
PRESS	4.18	1.635	1.930	2.400
r^2_{pred}	0.470	0.800	0.760	0.700
r^2_{bs}	0.977	0.956	0.955	0.935
Contributions (%)				
Steric	0.410		0.106	0.160
Electrostatic	0.590	0.470	0.420	0.552
Hydrophobic		0.280	0.249	
Donor		0.249	0.225	0.289

r^2_{cv} = cross-validated correlation coefficient; N = number of components; r^2 = conventional correlation coefficient; SEE = standard error of estimate; PRESS = predicted residual sum of squares of test set molecules, r^2_{pred} = predictive correlation coefficient, r^2_{bs} = correlation coefficient after 100 runs of bootstrapping analysis, S = steric field, E = electrostatic field, H = hydrophobic field, D = hydrogen bond donor field, A = hydrogen bond acceptor field.

original data set that are of the same size as the original. The same data can be sampled more than once. The statistical analysis is performed on each of the simulating data sets. The component model with consistent result is than chosen as the final model.The entire cross-validated results were analysed considering the fact that a value of r^2_{cv} above 0.3 indicates that probability of chance correlation is less than 5%.[9]

Predictive correlation coefficient[9]

The predictive ability of each 3D-QSAR model was determined from a set of ten compounds that were not included in the training set. These molecules were aligned, and their activities were predicted. The predictive correlation coefficient (r^2_{pred}), based on molecules of test set, is defined as,

$$r^2_{pred} = (SD - PRESS)/SD$$

where, standard deviation (SD) is the sum of the squared deviations between the biological activities of the test set and mean activities of the training set molecules and predictive residual sum of squares (PRESS) is the sum of squared deviation between predicted and actual activity values for every molecule in test set.

RESULTS

The CoMFA model obtained with 45 NAIMS derivatives in training set resulted in a six-component model with cross-validated correlation coefficient of 0.517 and minimum standard error. This analysis was used for final noncross validated run, giving a correlation coefficient of 0.965, giving a good linear correlation between the observed and predicted activities of the molecules in the training set.

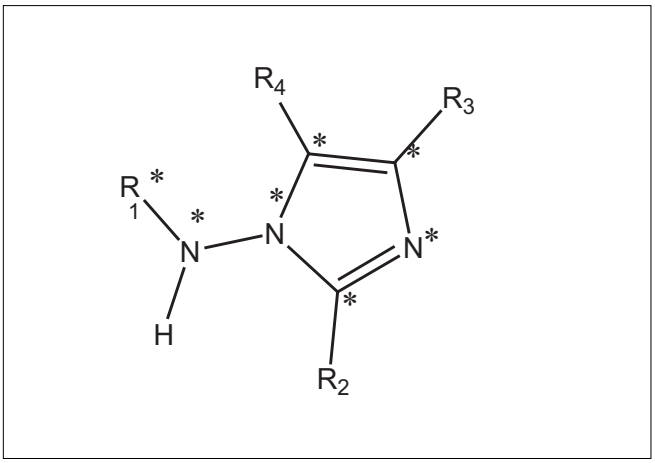

Figure 1: Novel NAIMS analogs used for 3D-QSAR studies (common substructure is labeled with*).

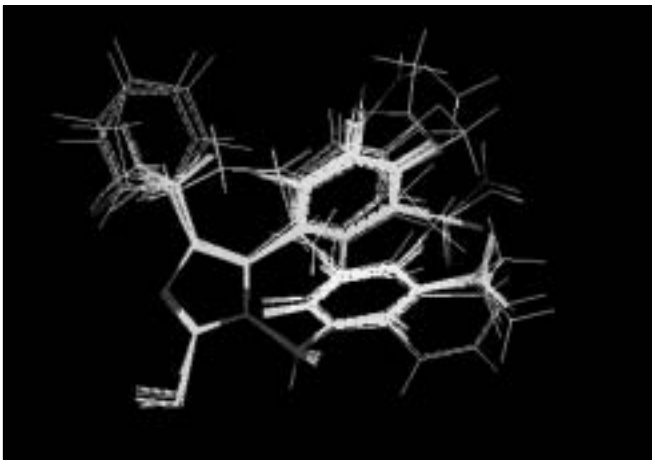

Figure 2: Alignment of the training set molecules

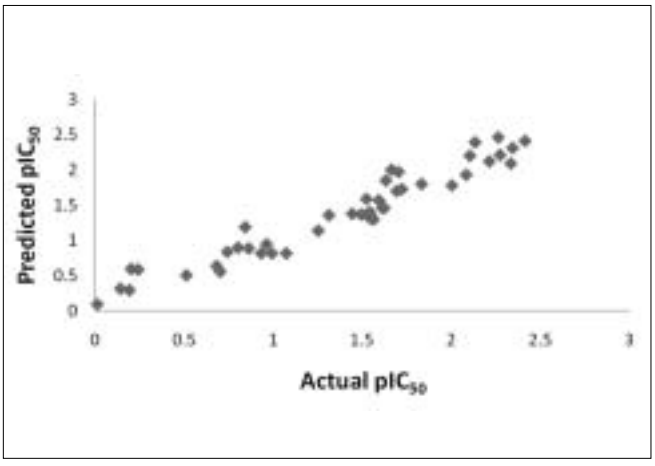

Figure 3: Plot of predicted versus actual pIC50 values of training set molecules for CoMFA model

To test the predictive ability of the resulting model, a test set of nine molecules excluded from the model creation work was used. The predictive correlation coefficient of 0.47 was obtained for CoMFA model. However, a high r^2 value of 0.977 during 100 runs of bootstrapped analysis further supports the statistical validity of the model. The alignment of the training set molecules is shown in Figure 2. The results of PLS analysis for CoMFA and CoMSIA are shown in Table 2. The relative contributions of steric and electrostatic fields for CoMFA are in the ratio 2:3. Electrostatic interactions of the molecule with active site of the enzyme could be an important factor for anti-HIV activity. A plot of predicted (CoMFA) versus actual activity for training set molecules is shown in Figure 3. Figure 4 represents the plot of predicted (CoMSIA) versus actual activity values, while the test set residuals of CoMFA and CoMSIA analyses are shown in Figure 5. Figure 6 represents the plot of cross validated correlation coefficient versus all the CoMSIA models. The actual, predicted and residual values of training and test set for CoMFA and CoMSIA are given in Tables 3 and 4, respectively. Contour maps were generated as scalar product of coefficients and SD associated with each CoMFA column. The 3D-QSAR contour maps revealing the contribution of CoMFA and

Table 3: Experimental and predicted activities of compounds in training set

Compd. No.	pIC50 experimental	pIC50 predicted		Residual activity	
		CoMFA	CoMSIA	CoMFA	CoMSIA
1	0.8	0.92	0.9	-0.12	-0.1
2	2.34	2.59	2.31	-0.25	0.03
3	2.13	2.26	2.39	-0.13	-0.26
4	0.93	0.85	0.82	0.08	0.11
5	1.52	1.54	1.37	-0.02	0.15
6	0.7	0.65	0.56	0.05	0.14
7	1.61	1.61	1.46	0	0.15
8	1.59	1.62	1.57	-0.03	0.02
9	1.70	1.78	1.97	-0.08	-0.27
10	2.1	2.12	2.2	-0.02	-0.1
11	0.99	0.85	0.82	0.14	0.17
12	0.86	0.76	0.89	0.1	-0.03
13	0.19	0.24	0.3	-0.05	-0.11
14	2.41	2.4	2.41	0.01	0
15	2.26	2.44	2.46	-0.18	-0.2
16	1.63	1.79	1.85	-0.16	-0.22
17	0.96	0.86	0.95	0.1	0.01
18	1.25	1.13	1.14	0.12	0.11
19	1.56	1.56	1.3	0	0.26
20	1.69	1.62	1.7	0.07	0.01
21	0.01	0.15	0.1	-0.14	0.09
22	0.68	0.75	0.64	-0.07	0.04
23	2	1.73	1.78	0.27	0.22
24	1.66	1.74	2	-0.08	-0.34
25	2.08	2.11	1.93	-0.03	0.15
26	2.27	2.19	2.21	0.08	0.06
27	1.62	1.50	1.46	0.12	0.16
28	0.74	0.76	0.84	-0.02	-0.1
29	1.54	1.62	1.35	-0.08	0.19
30	1.72	1.71	1.73	0.01	-0.01
31	0.2	0.49	0.6	-0.29	-0.4
32	0.24	0.26	0.59	-0.02	0.05
33	0.14	0.3	0.32	-0.16	-0.18
34	1.83	1.8	1.8	0.03	0.03
35	1.07	0.78	0.82	0.29	0.25
36	2.33	2.12	2.09	0.21	0.24
37	0.51	0.58	0.51	-0.07	-0.3
38	1.49	1.36	1.37	0.13	0.12
39	1.44	1.35	1.38	0.09	0.06
40	1.31	1.2	1.36	0.11	-0.05
41	1.54	1.47	1.32	0.07	0.22
42	0.84	0.95	1.19	-0.11	-035
43	1.54	1.46	1.40	0.08	0.14
44	2.21	2.17	2.12	0.04	0.09
45	1.52	1.61	1.59	-0.09	-0.07

[a]pIC_{50}= -log IC_{50}

Table 4: Experimental and predicted inhibitory activities of compounds in test set

Compd. No.	Actual pIC_{50}[a]	Predicted pIC_{50}[a]		Residual activity	
		CoMFA	CoMSIA	CoMFA	CoMSIA
46	2.17	1.27	1.44	0.90	0.73
47	2.56	2.21	2.32	0.35	0.24
48	2.28	2.64	1.96	0.36	0.32
49	1.83	1.69	1.45	0.14	0.38
50	2.54	2.28	2.40	0.26	0.14
51	2.49	2.21	2.32	0.28	0.17
52	2.03	1.80	1.96	0.23	0.07
53	2.42	1.37	1.65	1.05	0.77
54	2.20	0.86	1.80	1.34	0.40

[a]pIC_{50}= -log IC_{50}

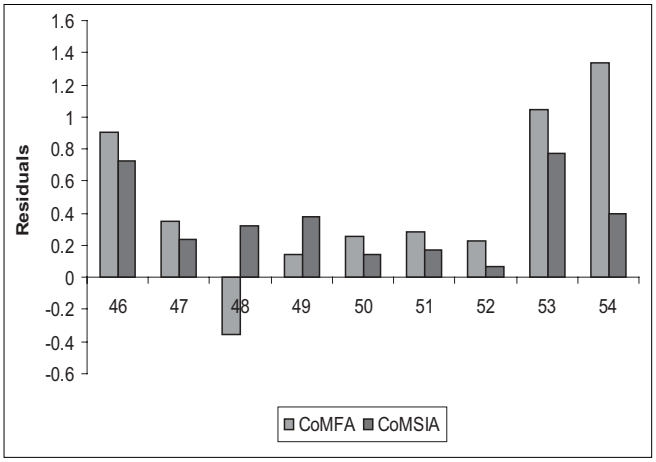

Figure 5: Histogram of test set molecules

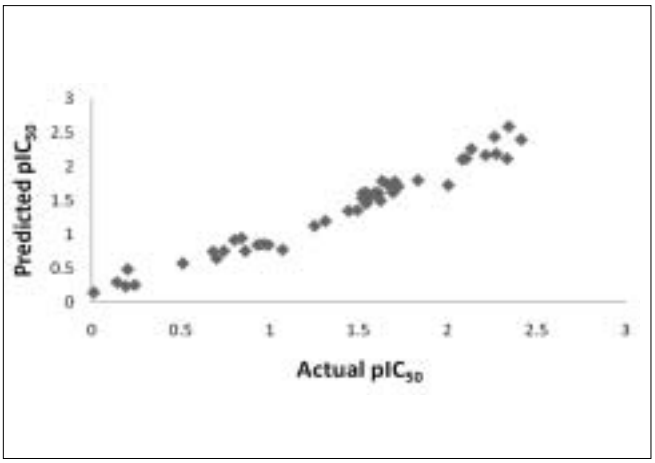

Figure 4: Plot of predicted versus actual pIC50 values of training set molecules for CoMSIA Model

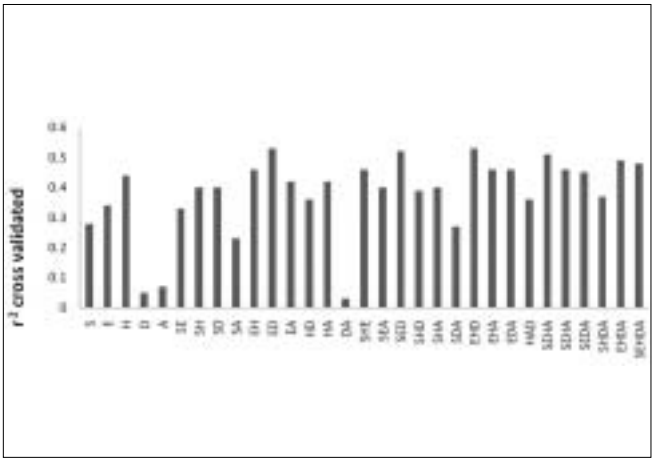

Figure 6: Plot of r2 cross validated versus different CoMSIA models

CoMSIA fields are shown in Figures 7 and 8, respectively.

DISCUSSION

The CoMFA steric interactions are represented by green (G) and yellow (Y) colored contours, while electrostatic interactions are represented by red (R) and blue (B) colored contours. The green contours represent the regions where bulky substituents are favored, while yellow contours represent regions of unfavorable steric effects. The blue contours depict the sites favoring positively charged groups and the red contours favor negatively charged groups. The most active molecule 13 [template molecule having highest activity against HIV-1-IIIB strain (IC_{50} = 1.56 ± 0.61)] is displayed in the background of contours. The electrostatic contours of CoMFA [Figure 7a] showed that the NH group attached to the first position of the imidazole moiety, the third position of the imidazole, as well as the *meta* position of the phenyl group on the fifth position of imidazole pharmacophore are surrounded by blue (B) contours exhibiting the need for electropositive groups. A big red (R) contour posed over the *meta* methyl group of the phenyl ring attached to the N^1-position indicates that biological activity can be enhanced by introduction of more electronegative groups at this position for strong electrostatic field interactions. Green (G) contours [Figure 7b] around the methyl group at the *meta* position of the phenyl group, attached to the NH side chain of the imidazole moiety indicates that substitution with bulky steric groups increases activity, while a big yellow (Y) contour surrounding the phenyl group at the fifth position of the imidazole nucleus shows that bulky groups are unfavorable. The CoMSIA results were obtained using the same structural alignment and same training and test set as defined in the CoMFA. Based on the predictive correlation coefficient (r^2_{pred} = 0.80), the combination of electrostatic, hydrophobic and hydrogen bond donor fields in CoMSIA gave the best results (Model 1), giving cross-validation correlation coefficient of 0.532 and a conventional correlation coefficient of 0.930. The other combinations such as (i) steric, electrostatic, hydrophobic

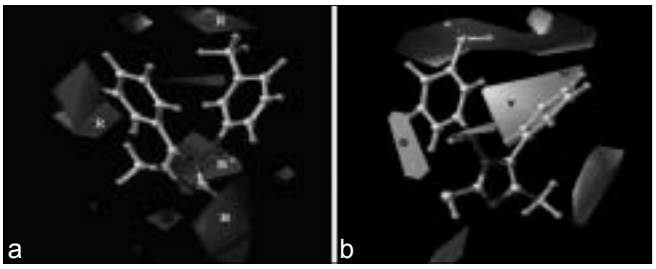

Figure 7: The CoMFA (a) steric and (b) electrostatic contour maps. One of the most active molecules 13 is shown in the background. Red (R) is a negatively charged region, blue (B) a positively charged region, green (G) a positive sterically active region, and yellow (G) a negative sterically active region

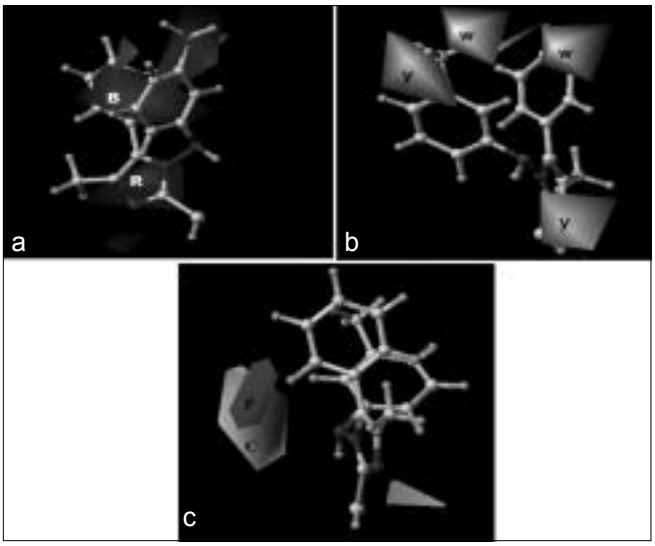

Figure 8: The CoMSIA electrostatic (a), hydrophobic (b) and hydrogen donor(c) contour maps. One of the most active molecules 13 is shown in the background. Red (R) is a negatively charged region, blue (B) a positively charged region, yellow (Y) a hydrophobically favored regions, white (W) hydrophobically disfavored regions, cyan(C) color is a hydrogen donor favoured region, and purple (P) color is a hydrogen donor disfavored region

and hydrogen bond donor fields (Model 2) and (ii) steric, electrostatic, and hydrogen bond donor fields (Model 3) in CoMSIA also gave statistically significant models. All other combinations in CoMSIA gave statistically insignificant results [Figure 6]. The Model 1 of CoMSIA was used for final analysis and predictions. A high r^2 value of 0.956 during 100 runs of bootstrapped analysis further supports the statistical validity and robustness of Model 1. The contributions of electrostatic, hydrophobic, and hydrogen bond donor fields of CoMSIA are in a ratio of 5:3:2 [Table 2]. When comparing the field contributions of the CoMFA analysis, it is revealed that electrostatic and hydrophobic interactions could be an important factor for anti-HIV activity. A comparison of the residuals of the models from CoMFA and CoMSIA is made to evaluate their predictive ability [Table 4]. Considering the electrostatic contours of CoMSIA (Model 1), the introduction of electronegative substituents in red (R) regions may increase the affinity while in blue (B) regions decrease the affinity. A comparison of the electrostatic contours produced by CoMFA and CoMSIA (Model 1) [Figures 7a and 8a], respectively, revealed that they are quite different. The analysis of electrostatic CoMSIA contours shows that the third and fourth position of the imidazole nucleus are embedded in a red (R) contour while a blue (B) contour surrounds the methyl group present at the *meta* position of the phenyl ring attached to the NH side chain of the imidazole nucleus. In hydrophobic contours, the yellow (Y) regions favour hydrophobic groups while white (W) regions favour hydrophilic groups.

The hydrophobic contours [Figure 8a] show that the thiol group at the second position of the imidazole moiety and the methyl group at the *meta* position of the phenyl group attached to the NH side chain are embedded in big yellow (Y) contours indicating that hydrophobic substituents at this position may increase the activity. The presence of a big white (W) contour around phenyl ring attached to the fifth position of imidazole nucleus indicates that hydrophobic substituents may decrease the activity at this position. In the hydrogen bond donor contours, cyan (C) contours indicate hydrogen bond donor favourable regions while purple (P) contours indicate hydrogen bond donor unfavourable regions for substituents. One small cyan (C) contour posed over the thiol group at the second position of the imidazole ring [Figure 8b] is seen where hydrogen bond donors may increase the activity whereas a purple contour on the second position of the phenyl group attached to the fifth position of imidazole ring show that donor groups at this position will decrease activity. The best CoMSIA model (Model 1) with a combination of electrostatic, hydrophobic and hydrogen bond donor fields indicates that steric and hydrogen bond acceptor fields do not improve the model. The CoMFA and CoMSIA models obtained from this study offer crucial information into the design of analogous NAIMS inhibitors with improved activity and selectivity and also for predicting their anti-HIV activity prior to chemical synthesis and biological testing.

CONCLUSION

The 3D-QSAR analyses, CoMFA, and CoMSIA have been applied to a set of NAIMS analogs active against HIV-1 IIIB strain. Statistically significant models with good correlative and predictive power for anti-HIV activities of the NAIMS analogs were obtained. The initial geometry of the template molecule (13, the most active of the

series against HIV-1 IIIB strain) was obtained from the simulated annealing approach and was then used to derive remaining structures. The robustness of the derived models was verified by bootstrapping method. The comparison of CoMFA and CoMSIA models revealed that the combination of electrostatic, hydrophobic, and hydrogen bond donor fields in CoMSIA gave the best results. Results of this study may be utilized for future drug design studies and synthesis of more potent anti-HIV agents using the NAIMS scaffold.

ACKNOWLEDGMENTS

One of the authors N. Prasanthi gratefully acknowledges the financial support to this work by UGC in the form of Junior Research Fellowship. The authors also wish to thank the financial assistance provided by the grant sanctioned under Research Promotion Scheme of AICTE, New Delhi.

REFERENCES

1. Clerque ED. HIV-chemotherapy and –prophylaxis: new drugs, leads and approaches. J Biochem Cell Biol 2004; 36:1800.
2. Maeda K, Osata T, Umezawa H. A new antibiotic, azomycin. J Antibiot (Tokyo) 1953; 6:182-4.
3. Ren J, Nichols C, Bird LE, Fujiwara T, Sugimoto H, Stuart DI, *et al*. Binding of the second generation non –nucleoside inhibitor S-1153 to HIV-1 reverse transcriptase involves extensive main chain hydrogen bonding. J Biol Chem 2000;275:14316-20.
4. Silvestri R, Martino GD. Synthesis, Biological Evaluation, and Binding Mode of Novel 1-[2-(Diarylmethoxy) ethyl]-2-methyl-5-nitroimidazoles Targeted at the HIV-1 Reverse Transcriptase. J Med Chem 2002;45:1567-76.
5. Sung YH, Kyu WK, Chung KR, Soo JK, Kwang HC. Antiproliferative effects of 6-anilino-5-chloro-1H-benzo[d]imidazole-4,7-dione in vascular smooth muscle cells. Bioorg Med Chem 2008;16:644–9.
6. Lagoja IM, Pannecouque C, Debyser Z, Balzarini J, Aerschot AV, Witvtouw M, *et al*. N-Aminoimidazole Derivatives Inhibiting Retroviral Replication via a Yet Unidentified Mode of Action. J Med Chem 2003;46:1546-53.
7. Kim KH, Comparative Molecular Field Analysis (CoMFA).In: Dean PM, editor. Molecular Similarity in Drug Design. Blackie Academic and Professional: London; 1995. p. 291-331.
8. Bohacek RS, McMartin CK. Definition and display of steric, hydrophobic, and hydrogen bonding properties of ligand binding sites in proteins using Lee and Richards accessible surface: validation of a high-resolution graphical tool for drug design. J Med Chem 1992;35:1671-84.
9. Chakroborti AK, Gopalakrishnan B, Sobhia ME, Malde AK. 3 D QSAR studies of indole derivatives as phosphodiesterase IV inhibitors. Eur J Med Chem 2003; 38:975-82.
10. Klebe G, Abraham U, Mietzner T. Molecular Similarity Indices in a Comparative Analysis (CoMSIA) of Drug Molecules to Correlate and Predict Their Biological Activity. J Med Chem 1994;37:4130-46.
11. K.Jasu, A.Basu, S.Bhattacharya, P.Ojha, Venkatesan.J, N.Mishra, Development of a COMFA and COMSIA model for cytotoxicity activity of Anti-HIV 1-Phenylamino-1H-imidazole Derivatives. European Journal Medicinal Chemistry, doi: 10.1016/j.ejmech.2008.09.043
12. SYBYL Molecular Modelling System, version 7.1, Tripos Associates, St. Louis, MO.

Source of Support: Nil, **Conflict of Interest:** None declared.